ELSEVIER

Contents lists available at ScienceDirect

European Journal of Pharmaceutical Sciences

journal homepage: www.elsevier.com/locate/ejps



Human enteroid monolayers as a potential alternative for Ussing chamber and Caco-2 monolayers to study passive permeability and drug efflux

Eva J. Streekstra ^{a,b}, Marit Keuper-Navis ^{b,c}, Jeroen J.M.W. van den Heuvel ^a, Petra van den Broek ^a, Martijn W.J. Stommel ^d, Sander Bervoets ^e, Luke O'Gorman ^e, Rick Greupink ^a, Frans G.M. Russel ^a, Evita van de Steeg ^{b,#}, Saskia N. de Wildt ^{a,f,g,#,*}

- ^a Division of Pharmacology and Toxicology, Department of Pharmacy, Radboud University Medical Center, P.O. Box 9101, 6500 HB Nijmegen (Route 137), Nijmegen, the Netherlands
- b Department of Metabolic Health Research, Netherlands Organization for Applied Scientific Research (TNO), Leiden, the Netherlands
- ^c Division of Pharmacology, Utrecht Institute for Pharmaceutical Sciences (UIPS), Utrecht University, Utrecht, the Netherlands
- ^d Department of Surgery, Radboud University Medical Center, Nijmegen, the Netherlands
- e Radboudumc Technology Center for Bioinformatics, Department of Medical BioSciences, Radboud University Medical Center, Nijmegen, the Netherlands
- ^f Department of Intensive Care, Radboud University Medical Center, Nijmegen, the Netherlands
- g Department of Neonatal and Pediatric Intensive Care, Erasmus MC Sophia Children's Hospital, Rotterdam, the Netherlands

ARTICLE INFO

Keywords: Pharmacokinetics Intestinal permeability Intestinal organoids Enteroids Ussing chamber Drug transport

ABSTRACT

After oral administration, the intestine is the first site of drug absorption, making it a key determinant of the bioavailability of a drug, and hence drug efficacy and safety. Existing non-clinical models of the intestinal barrier *in vitro* often fail to mimic the barrier and absorption of the human intestine. We explore if human enteroid monolayers are a suitable tool for intestinal absorption studies compared to primary tissue (Ussing chamber) and Caco-2 cells.

Bidirectional drug transport was determined in enteroid monolayers, fresh tissue (Ussing chamber methodology) and Caco-2 cells. Apparent permeability (P_{app}) and efflux ratios for enalaprilat (paracellular), propranolol (transcellular), talinolol (P-glycoprotein (P-gp)) and rosuvastatin (Breast cancer resistance protein (BCRP)) were determined and compared between all three methodologies and across intestinal regions. Bulk RNA sequencing was performed to compare gene expression between enteroid monolayers and primary tissue.

All three models showed functional efflux transport by P-gp and BCRP with higher basolateral to apical (B-to-A) transport compared to apical-to-basolateral (A-to-B). B-to-A P_{app} values were similar for talinolol and rosuvastatin in tissue and enteroids. Paracellular transport of enalaprilat was lower and transcellular transport of propranolol was higher in enteroids compared to tissue. Enteroids appeared show more region- specific gene expression compared to tissue.

Fresh tissue and enteroid monolayers both show active efflux by P-gp and BCRP in jejunum and ileum. Hence, the use of enteroid monolayers represents a promising and versatile experimental platform to complement current *in vitro* models.

1. Introduction

The intestine is a dynamic barrier involved in absorption and biotransformation of xenobiotic compounds, including drugs. After oral administration, the intestine is the first site of drug absorption, making it a key determinant of drug bioavailability and hence a drug's ultimate efficacy and safety. Elucidating its pharmacokinetic and toxicokinetic

drug interactions provides better guidance in safety assessment and can be used to understand and potentially also predict pharmacokinetics, *e. g.* using physiologically based pharmacokinetic (PBPK) modeling (Darwich et al., 2010; Harwood et al., 2013).

Compounds can pass the mucosal membrane passively or actively. Passive transport occurs transcellularly or paracellularly (through the tight junctions). Active transport of drugs is mediated by membrane

 $\hbox{\it E-mail address: $Saskia.dewildt@radboudumc.nl} \ (S.N.\ de\ Wildt).$

 $^{^{\}star}$ Corresponding author.

[#] E. van de Steeg and S.N. de Wildt share last authorship.

drug transporters (DTs), which can be uptake or efflux transporters (Alqahtani et al., 2021). P-glycoprotein (P-gp/ABCB1) and Breast Cancer Resistance Protein (BCRP/ABCG2) are the two major efflux transporters expressed in the intestinal barrier, both members of the ATP-binding cassette family and located on the apical membrane of the enterocyte (Estudante et al., 2013). Efflux transporters prevent compounds from entering the human body, protecting against exogenous compounds, hence limiting drug absorption by transporting them back into the intestinal lumen (Galetin et al., 2024). The expression of P-gp is known to increase along the small intestine, being highest in the ileum region but low again in the colon, while evidence for regional BCRP expression is currently contradictory (Drozdzik et al., 2019; Estudante et al., 2013; Muller et al., 2017; Terada and Hira, 2015).

In drug discovery the *in vitro* gold standard to study drug transport is the Caco-2 model, a human immortalized colon cancer cell line (Lu et al., 2022). Despite their wide use, Caco-2 cells lack the complexity of *in vivo* physiology as they do not display the interplay between different intestinal cell types, lack relevant metabolic enzyme expression and biological variation (Englund et al., 2006; Muller et al., 2017; Ölander et al., 2016). An alternative model to study intestinal drug transport is the Ussing chamber. In this *ex vivo* tissue preparation model, a piece of fresh intestinal tissue is mounted between two chambers enabling measurements of bidirectional drug transport over the intestinal barrier (Michiba et al., 2020; Rozehnal et al., 2012; Sjoberg et al., 2013; Streekstra et al., 2022). This methodology is technically demanding, time-consuming, while intestinal tissue availability is limited and when available also fragile and only viable for a short period of time.

Innovative approaches like tissue-derived organoids have the potential to better bridge the gap between in vitro studies and in vivo responses. In 2011, Sato et al., developed a technique to isolate stem cells from the human intestine and grow 3D structures called human intestinal organoids (enteroids) (Sato et al., 2011). These organoid models, derived directly from donor specific tissue, are self-organizing, multicellular complexes. Enteroids mimic many of the intestinal epithelium's key attributes, maintaining the (patho)physiological properties as genetic region specificity and disease characteristics of the original tissue (Fair et al., 2018; Jelinsky et al., 2022; Kraiczy et al., 2019; Meran et al., 2020; Michiba et al., 2022; Middendorp et al., 2014a). Initially, enteroids are grown in a 3D formation exhibiting the luminal site of the intestine on the inside, which makes the lumen inaccessible for drug exposure. Yet, enteroids can be grown in a monolayer formation creating an apical and basolateral surface, enabling the possibility to study drug interactions with transporters, metabolizing enzymes, and its barrier properties (Altay et al., 2019; Braverman and Yilmaz, 2018; Gunasekara et al., 2018; Kozuka et al., 2017; Scott et al., 2016; Speer et al., 2019b; Takenaka et al., 2016; Wang et al., 2017; Yamashita et al., 2021). This makes enteroid monolayers a promising model to study intestinal bidirectional drug transport and predict oral drug absorption.

The aim of this study was to explore the suitability of enteroid monolayers as an experimental platform for drug transport studies that complements the Ussing chamber and widely used Caco-2 cells. Moreover, we apply enteroid monolayers to demonstrate their applicability to study intestinal region-specific variation. We did this by comparing bidirectional transport of model compounds (enalaprilat, propranolol, talinolol, rosuvastatin) in enteroid monolayers with that in the Ussing chamber model, both in the jejunum and ileum region. In addition, we compared results from these systems with the conventional Caco-2 monolayer. Gene expression analysis was used to compare composition of enteroid monolayers and tissues using RNA sequencing to investigate whether enteroids have similar (regional related) expression patterns as their primary tissue.

2. Methodology

2.1. Human tissue

Left-over intestinal tissue was obtained from adult patients undergoing a pancreatoduodenectomy (proximal jejunum) or (right hemi) colectomy surgery (terminal ileum) at Radboud university medical center (Radboudumc), Nijmegen, the Netherlands from 2020 to 2023. No informed consent was needed for anonymous use of leftover material for research purpose, following the Dutch Code of Conduct for Responsible Use. The need for formal ethics approval was waived by the ethics committee of Radboudumc, Nijmegen, The Netherlands according to the Dutch Law on Human Research. Directly after surgical resection, tissue was put in ice cold Krebs buffer and transferred to the lab within 15 min. Part of the tissue was stored at 4 °C in supplemented Williams' E storage buffer for enteroid isolation (Table A.1), one part was immediately used for Ussing chamber experiments, while another part was snap frozen in liquid nitrogen for RNA analysis.

2.2. Cell culture

2.2.1. 3D enteroid culture

For the establishment of enteroids, crypts were isolated from tissue within 24 h after storage in transport buffer (jejunum n=5, ileum n=5). Procedures for generation and maintenance of enteroid cultures were based on STEMCELLTM Technologies IntestiCultTM protocol. Details on buffer and media compositions, including suppliers, are listed in Table A.1. In short, mucosal tissue was separated from muscle and serosa, cut into pieces of 2–3 mm and extensively washed with wash buffer. Next, tissue pieces were incubated for 1 hour in crypt releasing solution, after which crypts were collected from supernatant. Isolated crypts were suspended in Matrigel and seeded in 30 μ l droplets per well in a 48-well tissue culture plate, covered with 300 μ l Organoid Growth Medium. Medium was refreshed every 2–3 days and after 5–10 days cultures were mechanically passaged for culture continuation, or by enzymatic dissociation as described below for generation of enteroid monolayers.

2.2.2. 2D enteroids monolayers

Procedures of monolayer culture were based on STEMCELLTM Technologies IntestiCultTM protocol. To create enteroid monolayers, clear membrane inserts (6.5 mm, 0.4 μm pore size, Corning Costar 3470, STEMCELLTM Technologies, CELLTREAT #100–0997) were coated with collagen type I (rat tail) in 0.1% acetic acid for 1 hour at room temperature and subsequently washed with PBS. 3D enteroids (P1-P15) were collected in Advanced DMEM+++, centrifuged and made single cell with use of TripLE for 10 min, 37 °C and mechanical disruption. Cells were seeded on the permeable inserts in a concentration of 1×10^{5} cells/well in OGM, with medium refreshment every 2–3 days. Apical volume was 100 μl , basolateral volume 600 μl . When the monolayer confluency was confirmed by microscopy and Trans Epithelial Electrical Resistance (TEER) measurement, culture medium was changed to Organoid Differentiation Medium, refreshing every 2–3 days. After 5 days of differentiation, the bidirectional transport assay was performed.

2.2.3. Caco-2 monolayer

Human colorectal adenocarcinoma cells (Caco-2) (ATCC, Manassas, VA, USA) were cultured in a humidified incubator in supplemented DMEM (Table A.1). At 80% confluency cells were seeded on membrane inserts (1 \times 10 $^{-5}$ cells/well, 6.5 mm, 0.4 μ m pore size, Corning Costar 3470, STEMCELLTM Technologies, CELLTREAT #100–0997). Apical and basolateral medium was refreshed every 2–3 days. After 21 days of culture, the bidirectional transport assay was performed.

2.2.4. Bidirectional transport assay enteroid and Caco-2 monolayers

Drug transport experiments were performed in the apical to

basolateral (A-to-B, n=3) and basolateral to apical (B-to-A, n=3) direction. TEER was measured before every experiment in transport buffer (Table A.1). A drug cocktail (see section drug cocktail) was prepared in transport buffer and added to either the apical or basolateral side of the insert. Fluorescein-dextran 4 kDa (FD4, 50 μ M) was added to the apical side of each insert to monitor monolayer integrity during the experiment. Monolayers were put on a rocker (70 rpm) at 37 °C (Boj et al., 2021; Takenaka et al., 2014).Medium samples were taken at t=30, 60 and 120 min for drug analysis. After the experiment, integrity was examined by visual inspection (Olympus microscope) and FD4 leakage to the basolateral compartment (cut-off value $P_{app} < 1 \times 10^{-6}$ cm/s (Speer et al., 2019a).

2.2.5. Immunofluorescent staining

Immunofluorescent staining of monolayers was performed according to established protocol (STEMCELLTM Technologies). In short, monolayers were washed with PBS and fixed in paraformaldehyde for 1 hour, after which they were stored in PBS until use. To visualize monolayer morphology, inserts were incubated with blocking buffer (PBS containing 2% normal goat serum, 1% bovine serum albumin, 0.1% TritonTM X-100 and 0.05% Tween®20) at room temperature for 1 hour. After 3 times washing with PBS, Alexa FluorTM Plus 555 Phalloidin (Invitrogen, A30106) in PBS with 1% bovine serum albumin was added overnight at 4 °C. Inserts were washed again 3 times with PBS, incubated with DAPI in PBS (5 gm/ml) for 30 min at 4 °C and after a final wash with PBS mounted on a glass slide with ProLongTM Gold Antifade Mountant (Invitrogen). Images were acquired using Axio observer microscope (ZEISS) and processed with ZEN 2.3 pro (ZEISS).

2.3. Ussing chamber

Exact procedures and details used for the Ussing chamber studies with intestinal tissues were previously described by Streekstra & Kiss et al., 2022 (Streekstra et al., 2022). Additional details on buffers and culture medium composition are provided in Table A.1. In short, intestinal mucosal tissue was dissected from its muscle and serosal layers, after which it was vertically mounted between two chambers with an area of 0.71 cm 2 . The two chambers were filled with Krebs buffer with N-acetylcystein (700 µg/mL), which were kept at stable temperature of 37 °C and were carbonated continuously. Tissue viability was monitored by electrophysiology during the whole experiment. After 15–30 min of stabilization, the buffer was changed for prewarmed transport buffer containing a drug cocktail (see below) to start the bidirectional transport assay. Samples (50 µL) were taken at every 15 min up to two hours for drug analysis.

2.4. Drug cocktail for transport assays

Bidirectional drug transport in tissue and enteroid monolayers was evaluated using a cocktail of reference drugs, dosed on either apical or basolateral side. For passive transport via the transcellular route, propranolol (10 μ M, CAS: 13,071–11–9) was used (Roos et al., 2017). Enalaprilat (10 μ M, CAS: 84,680–54–6) was used as a barrier integrity marker as it is transported via the paracellular route (Sjoberg et al., 2013). To assess carrier-mediated efflux transport in both models, talinolol (2 μ M, CAS: 57,460–41–0) and rosuvastatin (5 μ M, CAS: 287, 714–41–4) were used as a substrate for P-gp and BCRP, respectively (Lee et al., 2015; Oswald et al., 2011).

2.5. LC-MS/MS analytical methods to analyze drug components

Drug concentrations were analyzed by liquid chromatography-tandem mass spectrometry (LC-MS/MS) with an Acquity ultraperformance liquid chromatography (UPLC; Waters, Milford, MA) coupled to a Xevo TQ- S (Waters) triple quadrupole mass spectrometer with a HSST3 analytical column (1.8 $\mu m; 100 \times 2.1$ mm, Acquity UPLC,

Waters, Ireland) according to previously described method(Streekstra et al., 2022)

2.6. Data analysis

The apparent permeability (P_{app}) was calculated for each substrate individually according to Eq. (1), where dQ/dt is the rate of drug transport from one half chamber to the other (either A-to-B or B-to-A, expressed in ng/s), A the exposed area of the tissue (cm²) and C_0 the initial concentration of the compound investigated in the donor compartment (ng/ml).

$$P_{app} = \left(\frac{dQ}{dt}\right) \times \left(\frac{1}{A \times C_0}\right) \tag{1}$$

Efflux ratios (ER) were determined according to Eq. (2). An efflux ratio \geq 2 indicates significant active efflux, were 1–2 is less determinate (FDA, 2020).

$$ER = \frac{P_{app, B-to-A}}{P_{app, A-to-B}} \tag{2}$$

2.7. Gene expression analysis

RNA-Seq analysis was performed on snap frozen intestinal tissue and differentiated enteroid monolayers cultured on permeable inserts, collected after bidirectional transport experiments. mRNA was isolated with the RNeasy Mini kit (Qiagen) according to the manufacturer's protocol. For preparation of RNA sequencing libraries the KAPA RNA HyperPrep kit with RiboErase (human/mouse/rat [HMR]) (Kapa Biosystems) was used according to previously published methodology (Geckin et al., 2023). For sequencing 59-bp paired-end reads were generated with the Illumina NextSeq 2000 instrument.

Trim Galore! v0.4.5 (Babraham Bioinformatics, Babraham, UK) was used for low-quality filtering of bases in RNA-Seq reads and adapter trimming, a tool for Cutadapt v1.18 and FastQC v0.11.8 (Babraham Bioinformatics). A human reference genome (GRCh38.95, Ensembl) was used to map genes using STAR v2.7.5a. Gene counts were calculated with HTSeq (v0.11.0) and an Ensembl GRCh38.95 GTF annotation file. Quality control was performed with MultiQC v1.7 to generate quality reports of all samples. Normalization and differential gene expression analysis was carried out in R v4.3.2 with DESeq2 v1.42.0. Pathway and GO term enrichment were performed with EnrichR v3.2 on selected genes (DESeq2 p-adjusted values < 0.05). Separate files on differential expressed transcripts in tissue and enteroid monolayers of the genes used in this publication are provided in Supplementary Table B.1. All gene counts are available upon request.

2.8. Statistical analysis

Data in the text and Table 1 are presented as median \pm inter quartile range (IQR). A Kruskal-Wallis with Dunn's post-hoc test, based on median \pm IQR, was applied to compare P_{app} for transport direction and differences between jejunum and ileum (Fig. 2A-D and 3A-D, Table A.2 and A.3). Efflux ratios were compared with Mann Whitney *t*-test based on mean ranks (Fig. 2E + 3E, Table A.4). Pairwise donor comparison between tissue and enteroids was performed with a Wilcoxon-signed rank test for B-to-A transport of talinolol and rosuvastatin (Fig. 4). Deseq normalized counts in jejunum and ileum were compared with a Kruskall-Wallis with Dunn's post-hoc test based on median \pm IQR (Fig. 4). All statistical analyses were performed using GraphPad Prism 8.0.1.

Table 1 Apparent permeability $(P_{app} x10-6 \text{ cm/s})$ and efflux ratio (ER) in median \pm IQR (n^*) determined in this study for tissue, enteroid monolayers and Caco-2 cells for the substrates enalaprilat, propranolol, talinolol and rosuvastatin.

			Enalaprilat (Paracellular)	Propranolol (Transcellular)	Talinolol (P-gp)	Rosuvastatin (BCRP)
Enteroid monolayers	Jejunum	A-to-B	0.2 ± 0.1 (5)	8 ± 2 (5)	0.1 ± 0.2 (5)	0.4 ± 0.1 (5)
		B-to-A	0.2 ± 0.1 (5)	15 ± 6 (5)	6 ± 2 (5)	3 ± 0.9 (5)
		ER	2 ± 2 (5)	2 ± 0.9 (5)	58 ± 116 (5)	9 ± 6 (5)
	Ileum	A-to-B	0.3 ± 0.2 (5)	7 ± 3 (5)	0.2 ± 0.2 (5)	0.3 ± 0.2 (5)
		B-to-A	0.4 ± 0.3 (5)	14 ± 4 (5)	8 ± 2 (5)	6 ± 3 (5)
		ER	2 ± 2 (5)	2 ± 0.4 (5)	28 ± 28 (5)	20 ± 18 (5)
Tissue	Jejunum	A-to-B	1 ± 1 (11)	1 ± 2 (11)	1 ± 1 (10)	1 ± 0.7 (9)
		B-to-A	$2\pm0.8~(11)$	2 ± 3 (13)	2 ± 3 (14)	$3 \pm 4 (11)$
		ER	1 ± 1 (9)	1 ± 1 (8)	3 ± 5 (9)	4 ± 3 (8)
	Ileum	A-to-B	2 ± 0.9 (4)	$4 \pm 2 (4)$	2 ± 1 (4)	$3 \pm 4 (4)$
		B-to-A	0.8 ± 2 (5)	2 ± 1 (6)	$4 \pm 2 (6)$	4 ± 11 (6)
		ER	0.8 ± 0.6 (4)	0.6 ± 0.2 (4)	3 ± 4 (4)	1 ± 1 (4)
Caco-2		A-to-B	0.2 ± 0.1 (3)	11 ± 6 (3)	0.2 ± 0.3 (3)	0.1 ± 0.2 (3)
		B-to-A	0.3 ± 0.2 (3)	$15 \pm 7 (3)$	$6 \pm 2 (3)$	8 ± 2 (3)
		ER	1 ± 2 (3)	1 ± 0.2 (3)	24 ± 28 (3)	$53 \pm 40 \ (3)$

^{*} n: number of individual donor experiments performed.

3. Results

3.1. Bidirectional drug transport in human intestinal enteroid monolayers

We established enteroid monolayers from 5 proximal jejunum and 5 terminal ileum donor tissues to investigate bidirectional drug transport across the intestinal barrier. Representative brightfield and immunofluorescent images are presented in Fig. 1. Accurate barrier formation

was confirmed by TEER, FD4 and enalaprilat transport (P_{app}) in luminal to basolateral direction (A-to-B) (Figure A.1).

The substrates enalaprilat and propranolol were selected as a control for passive transport via the paracellular and transcellular route, respectively. Paracellular enalaprilat transport (P_{app}) was comparable in both transport directions in both jejunum and ileum monolayers (Fig. 2A), indicating proper barrier formation. Propranolol transport was higher in B-to-A direction than A-to-B direction in ileum (Fig. 2B),

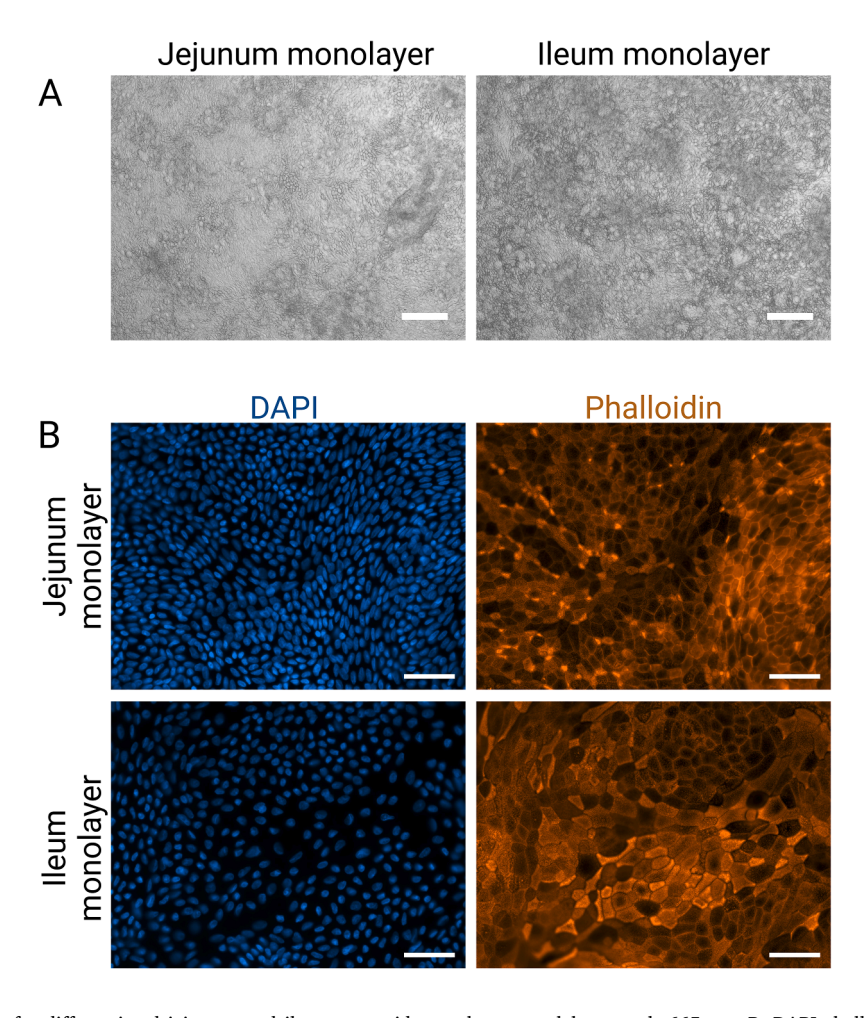


Fig. 1. A. brightfield images of a differentiated jejunum and ileum enteroid monolayers, scalebar equals 665 μm. B. DAPI-phalloidin staining of differentiated jejunum and ileum enteroid monolayers. In blue DAPI, in orange phalloidin, scalebar equals 50 μm.

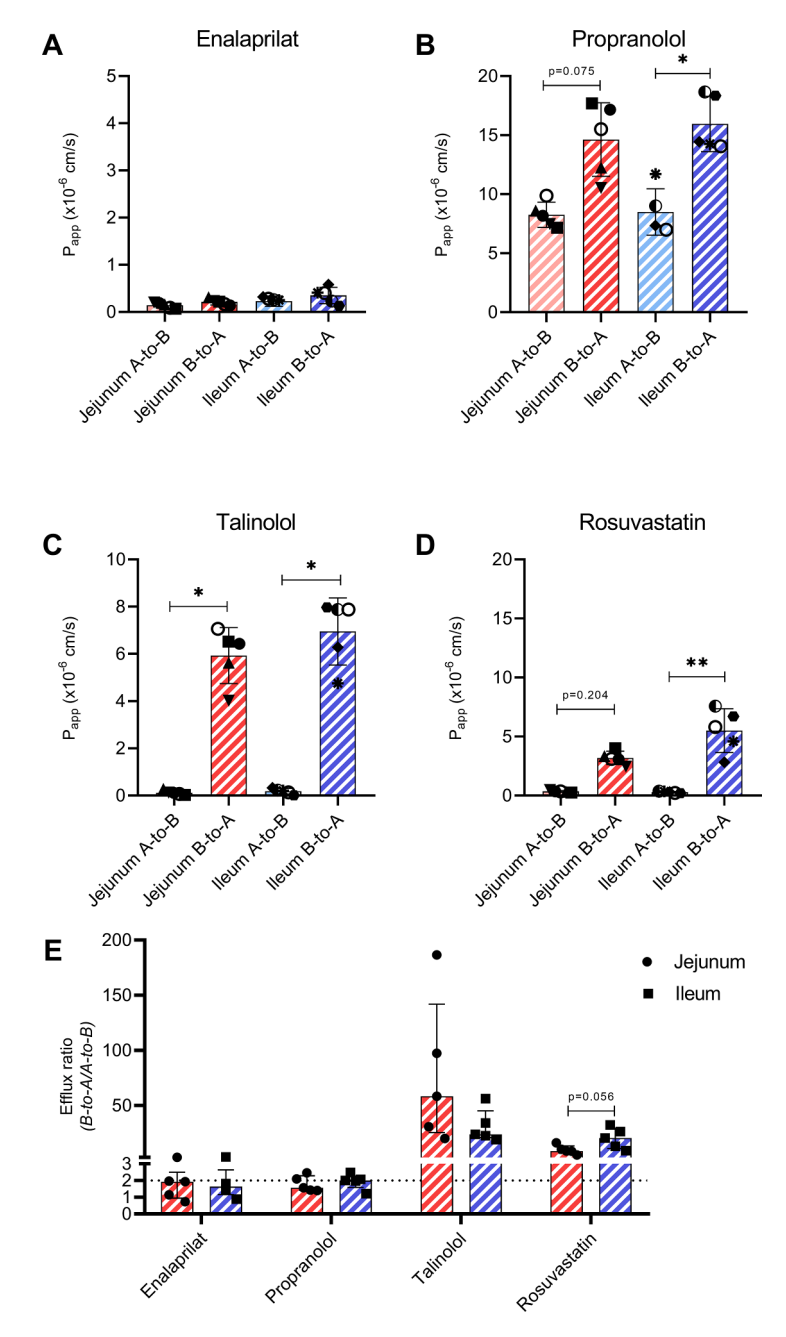


Fig. 2. apparent permeability (P_{app}) and related efflux ratios (ER) in enteroid monolayers in jejunum (circle) and ileum (square) for paracellular transport (enalaprilat), transcellular transport (propranolol) and active efflux by P-gp (P-glycoprotein, talinolol) and BCRP (Breast Cancer Resistance Protein, rosuvastatin). A-D: P_{app} in median \pm IQR, A-to-B = apical to basolateral transport. B-to-A = basolateral to apical transport. E: Efflux ratio median \pm IQR in jejunum (circle) and ileum (square). Dashed line indicates cut-off ratio of 2 for active efflux transport. Each symbol represents an individual donor. Open circle symbols do not have a paired donor sample in tissue or enteroid group.

resulting in ERs around 2 (Fig. 2E). No differences were apparent for P_{app} and ER of enalaprilat and propranolol between jejunum and ileum region nor for TEER and FD4 transport (Fig. 2, Figure A.1). Exact P_{app} values are presented in Table 1 and P-values can be found in Table A.2, A.3 and A.4.

In parallel, we evaluated drug transporter function by bidirectional talinolol (P-gp substrate) and rosuvastatin (BCRP substrate) transport across the enteroid monolayers. For talinolol the P_{app} in B-to-A direction was higher than A-to-B both in jejunum and ileum (Fig. 2C). Rosuvastatin transport was higher in B-to-A direction compared to A-to-B direction in ileum and showed the same trend in jejunum (Fig. 2D). For both substrates A-to-B transport was low (<0.5 \times 10 $^{-6}$ cm/s), also reflected by efflux ratios for talinolol and rosuvastatin that were all >>2

indicating functional P-gp and BCRP transport (Fig. 2E, Table 1). No significant difference was observed between jejunum and ileum in transport of talinolol and rosuvastatin. In addition, no regional effect was apparent in ER of talinolol (Fig. 2E). Efflux ratios for rosuvastatin however tended to be higher in ileum compared to jejunum (Fig. 2E, Table 1).

3.2. Bidirectional drug transport in human intestinal tissue

To compare bidirectional transport functionalities of enteroid monolayers and fresh intestinal tissue, we similarly studies transport in proximal jejunum (n=14) and terminal ileum (n=6) tissue explants in the Ussing chamber. Barrier integrity was monitored by TEER and FD4

transport (P_{app}) (Figure A.1).

The absorption rate of enalaprilat and propranolol in tissue was comparable in both transport directions and intestinal regions (Fig. 3A-B). Median efflux ratios for enalaprilat and propranolol were below 2 in both jejunum and ileum tissue, indicating passive transport of these substrates across the intestinal barrier (Fig. 3E, Table 1).

 P_{app} in B-to-A direction of talinolol tended to be higher than A-to-B transport in both jejunum and ileum (Fig. 3C, Table A.2). There was also a tendency of higher B-to-A transport of talinolol in the ileum tissue compared to jejunum tissue, suggesting higher activity of P-gp in ileum compared to jejunum, although this was not significant (Fig. 3C). The median efflux ratio of talinolol was >2 in 6 out of 9 experiments in jejunum and 2 out of 4 in ileum tissues, indicating active transport

(Fig. 3E). In jejunum tissue, rosuvastatin transport from B-to-A was higher compared to A-to-B (Fig. 3D), with a median ER > 2 in 7 out of 8 experiments indicating efflux transport (Table 1). Whereas in ileum large interindividual variation was observed, leading to inconclusive data (Fig. 3D).

3.3. Comparison of enteroid monolayers with Ussing chamber and Caco-2 monolayers

Subsequently, we compared enteroid monolayer derived P_{app} values and ER to the more conventional models; Ussing chamber and Caco-2 monolayers (Table 1, Supplementary Figure A.2 \pm 3). TEER measurements in enteroids showed variation between donors but median TEER

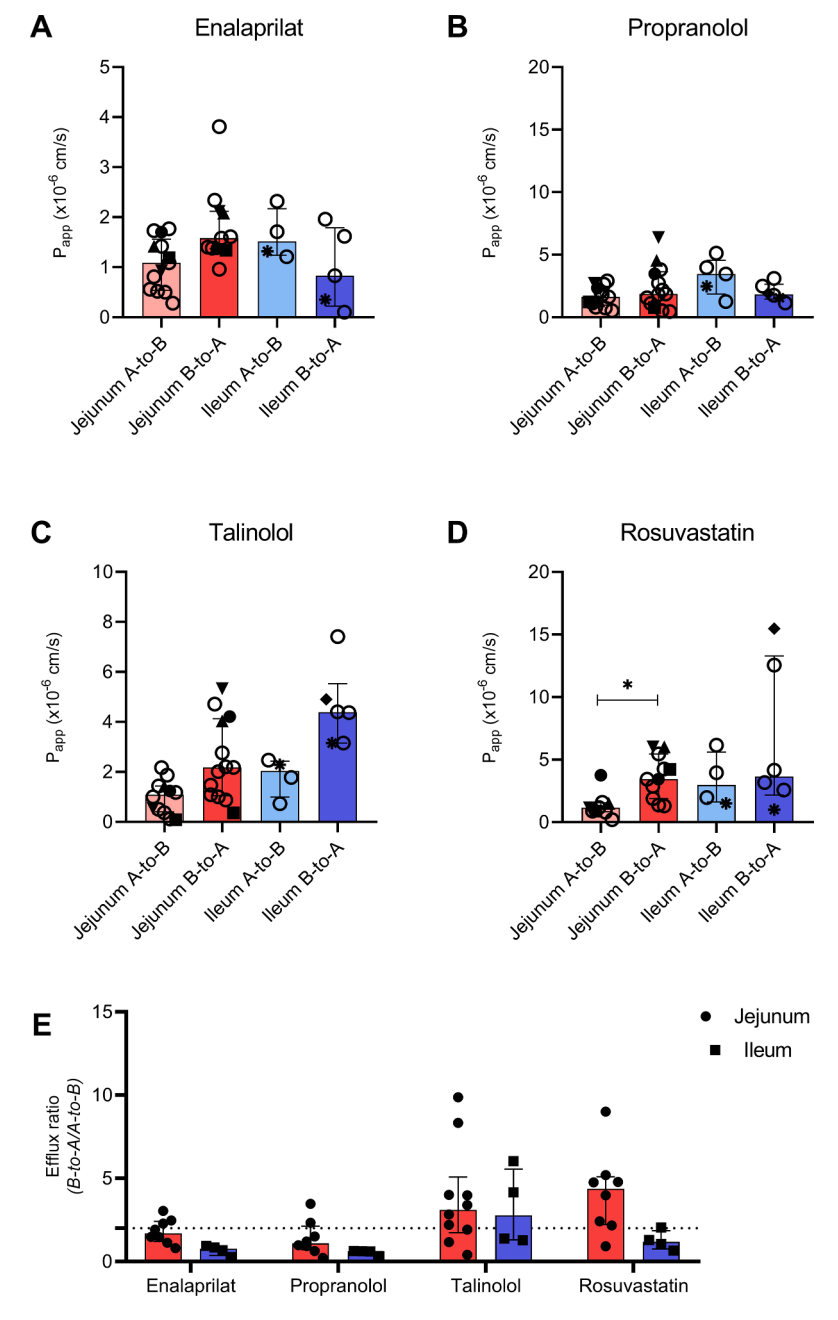


Fig. 3. Apparent permeability (P_{app}) and efflux ratios in tissue derived with the Ussing chamber in jejunum (circle) and ileum (square) for paracellular transport (enalaprilat), transcellular transport (propranolol) and active efflux by P-gp (P-glycoprotein, talinolol) and BCRP (Breast Cancer Resistance Protein, rosuvastatin). A-D: P_{app} in median \pm IQR, A-to-B = apical to basolateral transport. B-to-A = basolateral to apical transport. E: Efflux ratios in median \pm IQR in jejunum (circle) and ileum (square). Dashed line indicates cut-off ratio of 2 for active efflux transport. Each symbol represents an individual donor. Open circle symbols do not have a paired donor sample in tissue or enteroid group.

was similar to Caco-2, Ussing chamber TEER values were lower compared to the *in vitro* models (Figure A.1). No difference was observed in FD4 transport (P_{app}) between the *in vitro* models and tissue (Figure A.1).

For all models enalaprilat Papp and ER appeared similar between transport directions, with a tendency for the enteroids towards an ER around 2. A similar pattern was seen for propranolol transport. Nevertheless, enalaprilat Papp appeared lower and propranolol Papp higher in enteroid and Caco-2 monolayers compared to tissue, indicating differences between ex vivo and in vitro models (Table 1). For talinolol and rosuvastatin transport, A-B transport appeared 3- to 10-fold lower in enteroids and Caco-2, while B-to-A P_{app} values lay within the same range in comparison to tissue, resulting in high ERs. Pairwise donor comparison for P_{app} in B-to-A direction of talinolol and rosuvastatin can be found in Fig. 4. Most donor pairs show (in proportion) comparable Papp values in tissue as in enteroid monolayers. All model ERs are in line with active efflux by talinolol. The ER of talinolol in Caco-2 cells was in line with ileum enteroid monolayers. ERs for rosuvastatin appeared higher in Caco-2 compared to enteroids. Determined median Papp values and ERs are summarized in Table 1.

3.4. Intestinal gene expression in enteroids

To further explore if enteroid monolayers maintain tissue properties, we performed RNA sequencing on 3 jejunum and 7 ileum tissues as well as 3 jejunum-derived and 5 ileum-derived enteroid monolayers, of which 7 were paired donor samples. Based on global RNA expression profiles, enteroids monolayers and tissue were separated (PCA1: 86%) by principal component analysis (PCA). Intestinal regions were separated for both tissue (PC1: 41%) and enteroids (PC1: 46%) (Figure A.4). Expression profiles of proximal (GATA4) and distal (FABP6, GUCA2A, SLC10A2) gut markers confirmed the regional phenotype of the tissue and enteroids (Figure A.5) (Comelli et al., 2009; Middendorp et al., 2014a; Muller et al., 2017; Murata et al., 2023). We explored gene expression of transporters P-gp (ABCB1) and BCRP (ABCG2) in jejunum and ileum in both the tissue and enteroids. In both models, ABCB1 and ABCG2 were abundantly expressed. There appeared to be a trend of higher expression of ABCB1 and ABCG2 appears in ileum enteroids, compared to jejunum enteroids. In contrast, this difference was less well defined in tissue (Fig. 5). A Venn diagram of jejunum versus ileum in tissue and enteroid monolayers also showed more differentially expressed genes (DEGs) in enteroids compared to tissue, indicating that regional differences were more defined in enteroids (Fig. 6). A list with the exact DEGs in tissue and enteroid monolayers is provided in Supplementary Table C.1.

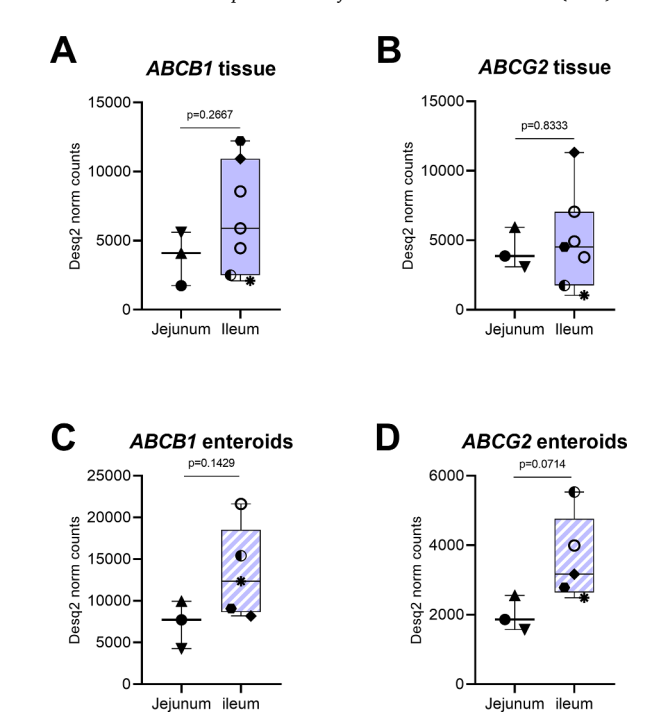


Fig. 5. Gene expression level counts normalized by DESeq2 of ABCB1 = P-gp, ABCG2 = BCRP. A+B expression in jejunum (n=3) and ileum (n=7) tissue, C + D expression in jejunum (n=3) and ileum (n=5) enteroid monolayers. Each symbol represents an individual donor. Open circle symbols do not have a paired donor sample in tissue or enteroid group.

4. Discussion

Enteroids can be successfully used to study patient-specific absorption pharmacokinetics and toxicokinetics. We have demonstrated the potential of enteroid monolayers derived from the jejunum and ileum as a promising test system for drug transport studies. Cultured 2D enteroids, Ussing chamber and Caco-2 cell studies all exhibited carrier mediated drug efflux by P-gp and BCRP. Moreover, the enteroids maintained trends of region of origin specific drug transport characteristics.

In this study, enteroid monolayers, Ussing chamber and Caco-2 reflected active transport by P-gp and BCRP, indicating a functional intestinal drug efflux barrier. Successful bidirectional transport studies were validated with TEER, FD4 transport, and the passive transport

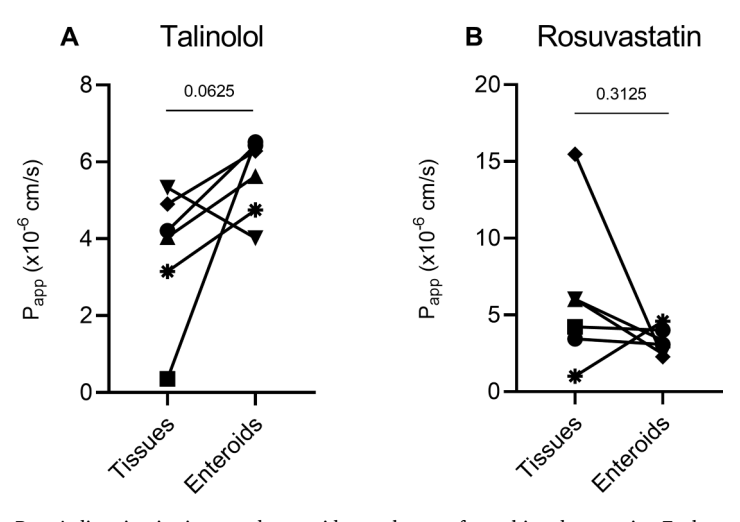


Fig. 4. Apparent permeability (P_{app}) in B-to-A direction in tissue and enteroid monolayers of matching donor pairs. Each symbol represents an individual donor. A. Talinolol. B. Rosuvastatin.

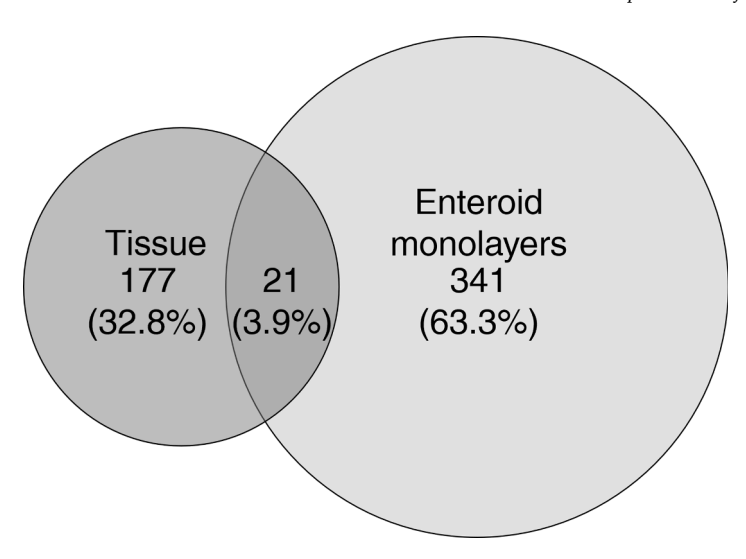


Fig. 6. Venn diagram differently expressed genes (DEGs) between jejunum (n = 3) and ileum (n = 7) in tissue and jejunum (n = 3) and ileum (n = 5) enteroid monolayers.

markers enalaprilat (paracellular) and propranolol (transcellular). B-to-A P_{app} values of talinolol and rosuvastatin fell within a similar range for the three different models and were mostly (in proportion) similar between paired tissue-enteroid donors. Some differences between tissue and enteroid monolayers derived data were observed, which need to be considered when using one of these models. Notably, paracellular transport (enalaprilat P_{app}) was lower in enteroids compared to tissue, as was A-to-B Papp for the efflux transporter substrates talinolol and rosuvastatin, i.e. the effect of the drug efflux transporters (ER) was more prominent in enteroids compared to tissue. The presence of numerous tight junctions in the in vitro monolayer model compared to tissue may account for both, as previously reported in Caco-2 cells by several studies (Artursson et al., 2001; Billat et al., 2017; Fedi et al., 2021). This was also reflected by the higher TEER values observed in enteroid and Caco-2 monolayers compared to fresh tissue (Figure A.1). Next to that, the unavoidable low stirring rate might not have been optimal for transcellular permeability of propranolol in enteroid monolayers. Loss of barrier integrity was observed when the stirring rate was increased, more research might be needed to improve this. To our knowledge, this is the first time that transport experiments in fresh tissue and enteroid monolayers were directly compared.

Several comparisons between enteroid monolayers and Caco-2 cells have been made before, but with major variation in enteroid origin and culture protocols. Previously, it has been shown that biopsy-derived enteroid monolayers more accurately recapitulate the intestinal tissue compared to Caco-2 considering the fraction absorbed and cytochrome P450 expression (Takenaka et al., 2016; Yamashita et al., 2021). Kourula et al. showed significantly higher efflux ratios for digoxin (P-gp substrate) and estrone-3-sulfate (BCRP substrate) in Caco-2 monolayers compared to biopsy-derived duodenal enteroid monolayers (Kourula et al., 2023). We show similar transport and ER of the P-gp substrate talinolol in Caco-2 and ileum enteroid monolayers. For BCRP we did observe a tendency of a higher efflux ratio in Caco-2 cells compared to enteroids. In addition, several reports show promising results for enteroids, such as a direct RNA expression comparison between an enterocyte monolayer derived from induced pluripotent stem cells (iPSC) to Caco-2 cells and biopsies, which showed more in vivo intestinal physiological similarities in iPSCs than in Caco-2 (Kwon et al., 2021; Takahashi et al., 2022).

In this study, enteroid monolayers and Ussing chamber experiments were performed with tissue from jejunum and ileum regions. It is known that gene expression levels of drug transporters differ among jejunum and ileum (Drozdzik et al., 2019; Matthew et al., 2019; Muller et al., 2017; Murata et al., 2023). Results in Fig. 2 and 3 show a potential

higher B-to-A transport (P_{app}) of talinolol in ileum compared to jejunum, although not significant, and also not reflected in ER. We did observe a higher efflux ratio of rosuvastatin by BCRP in ileum enteroid monolayers compared to the jejunum (Fig. 2). For rosuvastatin transport in ileum in the Ussing chamber system, inclusion numbers were low and P_{app} values were variable making it hard to draw conclusions on regional differences. Adjusting the *in vitro* culture characteristics to a more *in vivo* like microenvironment might improve regional drug transport even further, e.g. media adjustments, co-culture with commensal bacteria (Ahn et al., 2023; Puschhof et al., 2021).

Transport data derived with the Ussing chamber, especially in the Bto-A direction, are scarce in literature. It is important to note that the Ussing chamber method is known to manifest several challenges. The main limitation of this technique is the complexity of the methodology which is hard to perform in a consistent way, and experimental outcomes are dependent on tissue viability and handling, increasing interlaboratory variability (Sjoberg et al., 2013). For example, previously published Ussing chamber data showed varying results with large standard deviations for propranolol A-to-B transport in jejunum, Michiba et al., 2020, showed a P_{app} of 7.79 \pm 4.32 \times 10⁻⁶ cm/s (n = 6), Sjoberg et al., 2013, 31.9 \pm 17 \times 10⁻⁶ cm/s (n = 8), both higher compared to the P_{app} found in this study (1.4 \pm 0.8 \times 10⁻⁶ cm/s, n = 14) (Michiba et al., 2020; Sjoberg et al., 2013). Furthermore, in ileum previous data from our lab showed A-to-B 11.98 \pm 1.28 \times 10 $^{-6}$ cm/s in ileum compared to $2.9 \pm 1.0 \times 10^{-6}$ cm/s in this study (Streekstra et al., 2022). This shows the large variability of this methodology inter-laboratory and therefore makes it challenging to directly compare Ussing chamber and enteroid monolayer derived data. Nonetheless, in \emph{vivo} determined effective permeability ($P_{eff} \ x 10^{-4} \ cm/s)$ with Loc-I-gut or Triple-Lumen (clinical intestinal perfusion models) showed good correlation with fraction absorbed. The P_{eff} (mean $\pm \% \text{CV})$ for enalaprilat, propranolol and talinolol were 0.2 ± 150 , 3.2 ± 73 and 0.3 ± 171 , respectively, also emphasizing the variation in measurements (Dahlgren et al., 2015).

In addition to transport functionality, we examined mRNA expression through RNA sequencing in order to assess similarities between tissue and enteroids. We found more defined regional differences between jejunum and ileum in enteroids compared to tissues. Next, a trend was observed of higher expression of *ABCB1* and *ABCG2* in ileum compared to jejunum in enteroids (Fig. 4), which was less clear in tissue. The regional differences that were more pronounced in enteroids could be a result of *in vivo* cell extrinsic microenvironment disappearing upon *in vitro* culture, which depends more on cell intrinsic factors (Middendorp et al., 2014b). Our data support previous findings by Kraiczy

et al., who showed that terminal ileum and sigmoid colon enteroids retained their region-specific signature at both methylation and transcriptional level, and attributed this to the preserved epithelial-cell intrinsic factors *in vitro* (Kraiczy et al., 2019). They found more overlapping DEGs than we do, likely due to their use of EPCAM-sorted epithelial cells from tissue instead of whole tissue.

In this study, we performed bulk RNA sequencing has been performed on both fresh tissue and enteroid monolayers. The epithelial cell content of the samples taken was not measured before analysis. Hence, we cannot say that epithelial cell input was similar in all tissue samples, which may have influenced the variation between the samples. Future studies could consider cell sorting and single cell RNA sequencing (scRNAseq) for a more powerful analysis. scRNAseq would also provide a way to directly compare epithelial cell expression profiles in tissue with enteroids per cell type (Takayama et al., 2021).

Because of biological variation and donor-donor variation, increased donor numbers would help to strengthen the data and study regional variation and differences between the two models more robustly. More paired Ussing and enteroid monolayer derived data could offer more insight into interindividual variability in enteroids compared to tissue. Notably, it appears that the interindividual variation present in tissue is also represented in the enteroid monolayers. On the one hand this makes interpretation of results more challenging; on the other hand it provides opportunities. A good representation of existing biological variation makes the enteroid model more representative for the human situation and outcome predictions of clinical trials and modeling (Couto et al., 2020).

To summarize, enteroid monolayers and fresh tissue exhibit proper barrier function and active efflux by P-gp and BCRP. Biological variation within tissues and enteroids makes data interpretation challenging, but at the same time allows to include this variation in clinical drug transport research. Hence, the use of enteroid monolayers provide a versatile experimental platform that could complement or ultimately even replace current *in vitro* models as the widely used Caco-2 model.

Funding

This work was supported by the Radboudumc, Junior researcher round 2020, Nijmegen, The Netherlands.

CRediT authorship contribution statement

Eva J. Streekstra: Writing – original draft, Visualization, Resources, Methodology, Investigation, Formal analysis, Data curation, Conceptualization. Marit Keuper-Navis: Writing - review & editing, Visualization, Validation, Methodology, Investigation, Formal analysis. Jeroen J. M.W. van den Heuvel: Validation, Supervision, Methodology, Conceptualization. Petra van den Broek: Writing - original draft, Methodology. Martijn W.J. Stommel: Writing - review & editing, Resources, Methodology. Sander Bervoets: Writing - review & editing, Methodology, Formal analysis. Luke O'Gorman: Writing – review & editing, Software, Methodology, Formal analysis. Rick Greupink: Writing - review & editing, Supervision, Formal analysis. Frans G.M. Russel: Writing - review & editing, Supervision, Methodology, Conceptualization. Evita van de Steeg: Writing - review & editing, Supervision, Project administration, Investigation, Funding acquisition, Conceptualization. Saskia N. de Wildt: Writing - review & editing, Validation, Supervision, Resources, Project administration, Methodolacquisition, Investigation, Funding Data Conceptualization.

Declaration of competing interest

None.

Data availability

Data will be made available on request.

Supplementary materials

Supplementary material associated with this article can be found, in the online version, at doi:10.1016/j.ejps.2024.106877.

References

- Ahn, J.S., et al., 2023. Intestinal organoids as advanced modeling platforms to study the role of host-microbiome interaction in homeostasis and disease. BMB Rep. 56, 15–23. https://doi.org/10.5483/BMBRep.2022-0182.
- Alqahtani, M.S., et al., 2021. Advances in oral drug delivery. Front. Pharmacol. 12, 618411 https://doi.org/10.3389/fphar.2021.618411.
- Altay, G., et al., 2019. Self-organized intestinal epithelial monolayers in crypt and villuslike domains show effective barrier function. Sci. Rep. 9, 10140. https://doi.org/ 10.1038/s41598-019-46497-x.
- Artursson, P., et al., 2001. Caco-2 monolayers in experimental and theoretical predictions of drug transport1PII of original article: S0169-409X(96)00415-2. The article was originally published in Advanced Drug Delivery Reviews 22 (1996) 67–84.1. Adv. Drug Del. Rev. 46, 27–43. https://doi.org/10.1016/S0169-409X(00) 00128-9.
- Billat, P.A., et al., 2017. Models for drug absorption from the small intestine: where are we and where are we going? Drug Discov. Today 22, 761–775. https://doi.org/ 10.1016/j.drudis.2017.01.007.
- Boj, S.F., et al., 2021. Organoid-derived epithelial monolayer: a clinically relevant in vitro model for intestinal barrier function. JoVE e62074. https://doi.org/10.3791/ 62074
- Braverman, J., Yilmaz, O.H., 2018. From 3D organoids back to 2D enteroids. Dev. Cell 44, 533–534. https://doi.org/10.1016/j.devcel.2018.02.016.
- Comelli, E.M., et al., 2009. Biomarkers of human gastrointestinal tract regions. Mamm. Genome 20, 516–527. https://doi.org/10.1007/s00335-009-9212-7.
- Couto, N., et al., 2020. Quantitative proteomics of clinically relevant drug-metabolizing enzymes and drug transporters and their intercorrelations in the human small intestine. Drug Metab. Dispos. 48, 245–254. https://doi.org/10.1124/ dmd.119.089656.
- Dahlgren, D., et al., 2015. Direct in vivo human intestinal permeability (Peff) determined with different clinical perfusion and intubation methods. J. Pharm. Sci. 104, 2702–2726. https://doi.org/10.1002/jps.24258.
- Darwich, A.S., et al., 2010. Interplay of metabolism and transport in determining oral drug absorption and gut wall metabolism: a simulation assessment using the "Advanced Dissolution, Absorption, Metabolism (ADAM)" model. Curr. Drug Metab. 11, 716–729. https://doi.org/10.2174/138920010794328913.
- Drozdzik, M., et al., 2019. Protein abundance of clinically relevant drug transporters in the human liver and intestine: a comparative analysis in paired tissue specimens. Clin. Pharmacol. Ther. 105, 1204–1212. https://doi.org/10.1002/cpt.1301.
- Englund, G., et al., 2006. Regional levels of drug transporters along the human intestinal tract: co-expression of ABC and SLC transporters and comparison with Caco-2 cells. Eur. J. Pharm. Sci. 29, 269–277. https://doi.org/10.1016/j.ejps.2006.04.010.
- Estudante, M., et al., 2013. Intestinal drug transporters: an overview. Adv. Drug Deliv. Rev. 65, 1340–1356. https://doi.org/10.1016/j.addr.2012.09.042.
- Fair, K.L., et al., 2018. Intestinal organoids for modelling intestinal development and disease. Philos. Trans. R. Soc. Lond. B Biol. Sci. 373 https://doi.org/10.1098/ rstb.2017.0217.
- FDA, 2020. In Vitro Drug Interaction Studies Cytochrome P450 Enzyme- and Transporter-Mediated Drug Interactions. Food and Drug Administration.
- Fedi, A., et al., 2021. In vitro models replicating the human intestinal epithelium for absorption and metabolism studies: a systematic review. J. Controlled Rel. 335, 247–268. https://doi.org/10.1016/j.jconrel.2021.05.028.
- Galetin, A., et al., 2024. Membrane transporters in drug development and as determinants of precision medicine. Nat. Rev. Drug Discov. https://doi.org/ 10.1038/s41573-023-00877-1.
- Geckin, B., et al., 2023. Differences in immune responses in individuals of Indian and European origin: relevance for the COVID-19 pandemic. Microbiol. Spectr. 11, e0023123 https://doi.org/10.1128/spectrum.00231-23.
- Gunasekara, D.B., et al., 2018. A monolayer of primary colonic epithelium generated on a scaffold with a gradient of stiffness for drug transport studies. Anal. Chem. 90, 13331–13340. https://doi.org/10.1021/acs.analchem.8b02845.
- Harwood, M.D., et al., 2013. Absolute abundance and function of intestinal drug transporters: a prerequisite for fully mechanistic in vitro—in vivo extrapolation of oral drug absorption. Biopharm. Drug Disposit. 34, 2–28. https://doi.org/10.1002/ bdd.1810.
- Jelinsky, S.A., et al., 2022. Molecular and functional characterization of human intestinal organoids and monolayers for modeling epithelial barrier. Inflamm. Bowel Dis. 29, 195–206. https://doi.org/10.1093/ibd/izac212.
- Kourula, S., et al., 2023. Intestinal organoids as an *in vitro* platform to characterize disposition, metabolism, and safety profile of small molecules. Eur. J. Pharm. Sci. 188, 106481 https://doi.org/10.1016/j.ejps.2023.106481.

- Kozuka, K., et al., 2017. Development and characterization of a human and mouse intestinal epithelial cell monolayer platform. Stem Cell Rep. 9, 1976–1990. https:// doi.org/10.1016/j.stemcr.2017.10.013.
- Kraiczy, J., et al., 2019. DNA methylation defines regional identity of human intestinal epithelial organoids and undergoes dynamic changes during development. Gut 68, 49–61. https://doi.org/10.1136/gutjnl-2017-314817.
- Kwon, O., et al., 2021. The development of a functional human small intestinal epithelium model for drug absorption. Sci. Adv. 7 https://doi.org/10.1126/sciadv. abh1586.
- Lee, C.A., et al., 2015. Breast cancer resistance protein (ABCG2) in clinical pharmacokinetics and drug interactions: practical recommendations for clinical victim and perpetrator drug-drug interaction study design. Drug Metab. Disposit. 43, 490. https://doi.org/10.1124/dmd.114.062174.
- Lu, R., et al., 2022. Strategies and mechanism in reversing intestinal drug efflux in oral drug delivery. Pharmaceutics. 14 https://doi.org/10.3390/pharmaceutics14061131.
- Matthew, D.H., et al., 2019. The regional-specific relative and absolute expression of gut transporters in adult caucasians: a meta-analysis. Drug Metab. Disposit. 47, 854. https://doi.org/10.1124/dmd.119.086959.
- Meran, L., et al., 2020. Engineering transplantable jejunal mucosal grafts using patient-derived organoids from children with intestinal failure. Nat. Med. 26, 1593–1601. https://doi.org/10.1038/s41591-020-1024-z.
- Michiba, K., et al., 2020. Characterization of the human intestinal drug transport with Ussing chamber system incorporating freshly-isolated human jejunum. Drug Metab. Dispos. https://doi.org/10.1124/dmd.120.000138.
- Michiba, K., et al., 2022. Usefulness of human Jejunal spheroid-derived differentiated intestinal epithelial cells for the prediction of intestinal drug absorption in humans. Drug Metab. Dispos. 50, 204–213. https://doi.org/10.1124/dmd.121.000796.
- Middendorp, S., et al., 2014a. Adult stem cells in the small intestine are intrinsically programmed with their location-specific function. Stem Cells (1981) 32, 1083–1091. https://doi.org/10.1002/stem.1655.
- Middendorp, S., et al., 2014b. Adult stem cells in the small intestine are intrinsically programmed with their location-specific function. Stem Cells (1981) 32, 1083–1091.
- Muller, J., et al., 2017. Expression, regulation and function of intestinal drug transporters: an update. Biol. Chem. 398, 175–192. https://doi.org/10.1515/hsz-2016-0259.
- Murata, M., et al., 2023. Regional transcriptomics and proteomics of pharmacokinetics-related genes in human intestine. Mol. Pharm. 20, 2876–2890. https://doi.org/10.1021/acs.molpharmaceut.2c01002.
- Ölander, M., et al., 2016. The proteome of filter-grown Caco-2 cells with a focus on proteins involved in drug disposition. J. Pharm. Sci. 105, 817–827. https://doi.org/ 10.1016/j.xphs.2015.10.030.
- Oswald, S., et al., 2011. In vivo probes of drug transport: commonly used probe drugs to assess function of intestinal P-glycoprotein (ABCB1) in humans. In: Fromm, M.F., Kim, R.B. (Eds.), Drug Transporters. Springer Berlin Heidelberg, Berlin, Heidelberg, pp. 403–447.
- Puschhof, J., et al., 2021. Intestinal organoid cocultures with microbes. Nat. Protoc. 16, 4633–4649. https://doi.org/10.1038/s41596-021-00589-z.

- Roos, C., et al., 2017. Regional intestinal permeability in rats: a comparison of methods. Mol. Pharm. 14, 4252–4261, https://doi.org/10.1021/acs.molpharmaceut.7b00279.
- Rozehnal, V., et al., 2012. Human small intestinal and colonic tissue mounted in the Ussing chamber as a tool for characterizing the intestinal absorption of drugs. Eur. J. Pharm. Sci. 46, 367–373. https://doi.org/10.1016/j.ejps.2012.02.025.
- Sato, T., et al., 2011. Long-term expansion of epithelial organoids from human colon, adenoma, adenocarcinoma, and Barrett's epithelium. Gastroenterology 141, 1762–1772. https://doi.org/10.1053/j.gastro.2011.07.050.
- Scott, A., et al., 2016. Long-term renewable human intestinal epithelial stem cells as monolayers: a potential for clinical use. J. Pediatr. Surg. 51, 995–1000. https://doi. org/10.1016/j.jpedsurg.2016.02.074.
- Sjoberg, A., et al., 2013. Comprehensive study on regional human intestinal permeability and prediction of fraction absorbed of drugs using the Ussing chamber technique. Eur. J. Pharm. Sci. 48, 166–180. https://doi.org/10.1016/j.ejps.2012.10.007.
- Speer, J.E., et al., 2019a. Molecular transport through primary human small intestinal monolayers by culture on a collagen scaffold with a gradient of chemical crosslinking. J. Biol. Eng. 13, 36. https://doi.org/10.1186/s13036-019-0165-4.
- Speer, J.E., et al., 2019b. Evaluation of human primary intestinal monolayers for drug metabolizing capabilities. J. Biol. Eng. 13, 82. https://doi.org/10.1186/s13036-019-0212-1
- Streekstra, E.J., et al., 2022. A proof of concept using the Ussing chamber methodology to study pediatric intestinal drug transport and age-dependent differences in absorption. Clin. Transl. Sci. 15, 2392–2402. https://doi.org/10.1111/cts.13368.
- Takahashi, Y., et al., 2022. Organoid-derived intestinal epithelial cells are a suitable model for preclinical toxicology and pharmacokinetic studies. iScience 25, 104542. https://doi.org/10.1016/j.isci.2022.104542.
- Takayama, K., et al., 2021. In vivo gene expression profile of human intestinal epithelial cells: from the viewpoint of drug metabolism and pharmacokinetics. Drug Metab. Dispos. 49, 221–232. https://doi.org/10.1124/dmd.120.000283.
- Takenaka, T., et al., 2014. Human small intestinal epithelial cells differentiated from adult intestinal stem cells as a novel system for predicting oral drug absorption in humans. Drug Metab. Disposit. 42, 1947–1954. https://doi.org/10.1124/ dmd.114.059493.
- Takenaka, T., et al., 2016. Application of a human intestinal epithelial cell monolayer to the prediction of oral drug absorption in humans as a superior alternative to the Caco-2 cell monolayer. J. Pharm. Sci. 105, 915–924. https://doi.org/10.1016/j.xphs.2015.11.035.
- Terada, T., Hira, D., 2015. Intestinal and hepatic drug transporters: pharmacokinetic, pathophysiological, and pharmacogenetic roles. J. Gastroenterol. 50, 508–519. https://doi.org/10.1007/s00535-015-1061-4.
- Wang, Y., et al., 2017. Self-renewing monolayer of primary colonic or rectal epithelial cells. Cell. Mol. Gastroenterol. Hepatol. 4, 165–182. https://doi.org/10.1016/j. jcmgh.2017.02.011 e167.
- Yamashita, T., et al., 2021. Monolayer platform using human biopsy-derived duodenal organoids for pharmaceutical research. Mol. Ther. - Methods Clin. Dev. 22, 263–278. https://doi.org/10.1016/j.omtm.2021.05.005.